ARCHIVES OF MECHANICS
Arch. Mech. **76** (5), 389–412, 2024, DOI: 10.24423/aom.4494

# Buckling and post-buckling analysis of FGM plates resting on the two-parameter Vlasov foundation using general third-order plate theory

M. TACZAŁA[1)], R. BUCZKOWSKI[1)], M. KLEIBER[2)]

[1)] *West Pomeranian University of Technology in Szczecin, Faculty of Maritime Technology and Transport, Piastów 41, 71-065 Szczecin, Poland, e-mails: maciej.taczala@zut.edu.pl (corresponding author), rbuczkowski@ps.pl*

[2)] *Institute of Fundamental Technological Research, Polish Academy of Sciences, Pawińskiego 5B, 02-106 Warsaw, Poland, e-mail: mkleiber@ippt.pan.pl*

We present a nonlinear finite element analysis to investigate the buckling and post-buckling behaviour of functionally graded material (FGM) plates resting on the elastic foundation. The material properties are assumed to vary gradually across the thickness according to a power law distribution. The starting point of the investigation is the generalized third-order plate theory and the Vlasov model of elastic foundation having properties varying throughout the depth. The plates are subjected to bending to verify the formulation and compression loads including buckling and post-buckling analysis to investigate the influence of various parameters on the structural response.

**Key words:** FGM plate, elastic foundation, post-buckling, nonlinear finite element analysis.



## 1. Introduction

Functionally graded materials (FGMs) are inhomogeneous composite materials in which the volume fraction of two components varies smoothly and continuously across the given direction. FGMs are mixtures of ceramics and metal, where external ceramic layers due to large thermal resistance are exposed to high temperatures, while internal metallic constituents, owing to their stronger mechanical performance, are able to reduce the possibility of fracture. Manufacturing techniques must guarantee controlled changes in composition and density, so that the product will have a required structure and properties along the given direction, typically across the plate thickness. In recent years many articles concerned with the mechanics of functionally graded plates have been published. Usually new analysis methods are developed to handle the continuous variation in material properties through the thickness of the plate and extensive results are presented.

Various aspects of behaviour of the FGM plates have been studied by many researchers as reported by Swaminathan *et al.* [1, 2] while the review of the buckling and postbuckling of FGM plates can be found in [3] and [4].

Javaheri and Eslami [5] investigated the buckling of functionally graded plates under in-plane compressive loading. Shariat and Eslami [6] studied the buckling of thick functionally graded plates under mechanical and thermal loading. Prakash *et al.* [7] used an eight-nodded $C^0$ shear flexible quadrilateral plate element to study the nonlinear bending/pseudo-post-buckling behaviour of FGM plates based on the Mindlin formulation under thermo-mechanical load and concluded that temperature dependent material properties overestimates the thermal postbuckling resistance. Later, Prakash *et al.* [8] extended their investigations to study the influence of the position of the neutral surface on the stability behaviour of FGM plates. The conditions for the bifurcation-type buckling were examined by Aydogdu [9]. He observed that this type of buckling occurs when the plate is fully clamped while for simply supported plate edges the condition is to apply the loading at the neutral surface. Lee *et al.* [10], based on the first-order shear deformation plate theory (FSDT), studied the postbuckling behavior of unstiffened FGM plates under edge compression and temperature field conditions using the element-free kp-Ritz method. Zenkour and Sobhy [11] studied the thermal buckling of functionally graded material plates using the sinusoidal shear deformation plate theory. Duc and Van Tung [12] analytically investigated buckling and post-buckling behaviour of thick functionally graded plates resting on elastic foundations and subjected to in-plane compressive, thermal and thermomechanical loads. Their formulations were based on the higher order shear deformation plate theory taking into account the von Kármán nonlinearity, initial geometrical imperfection and the Pasternak type elastic foundation.

Bodaghi and Saidi [13] used the neutral surface based-CPT to study the buckling of FG plates resting on an elastic foundation under non-uniform compression. Based on the third-order shear deformation theory, Akbarzadeh *et al.* [14] obtained the results for the behaviour of FGM plates under lateral thermal shock using the couple thermoelastic assumption.

A similar approach was applied by Kowal-Michalska and Mania [15] who investigated the static and dynamic buckling of FG plates subjected to a simultaneous action of one directional compression and thermal loadings. Zhang [16] used the Ritz energy method to study the nonlinear post-buckling, nonlinear bending and vibration of FGM plates based on physical neutral surface and Reddy's third-order shear deformation. Latifi *et al.* [17] used the classical plate theory based on physical neutral surface expanding the displacement functions in the double Fourier series to investigate the buckling behaviour of FGM plates subjected to proportional biaxial compressive loadings. Thai and Uy [18] applied the refined plate theory to derive analytical solutions for the buckling load of FG Levy-type plates based on the neutral surface. Mansouri and Shariyat [19] analysed thermo-mechanical buckling of the orthotropic auxetic plates in the hygrothermal environments solving the high-order shear-deformation governing differential equations using the new differential quadrature method. Han *et al.* [20] investigated the dynamic instability analysis of S-FGM (sigmoid FGM) on an elastic medium using the third-order shear deformation theory. Lee *et al.* [21] analysed the thermal buckling behaviour of functionally graded plates based on FSDT and neutral surface of structures. Fan and Wang [22] investigated nonlinear bending and post-buckling behaviour of a hybrid laminated plate resting on the Pasternak elastic foundation in thermal environments. The plate was composed of conventional fiber reinforced composite (FRC) layers and carbon nanotube reinforced composite (CNTRC) layers. Chikh *et al.* [23] presented an analytical formulation based on both hyperbolic shear deformation theory and stress function to study the nonlinear post-buckling response of symmetric functionally graded plates supported by elastic foundations and subjected to in-plane compressive, thermal and thermo-mechanical loads.

Shams *et al.* [24] analysed the buckling behaviour of functionally graded carbon nanotube-reinforced composite (FG-CNTRC) plates resting on the Winkler–Pasternak elastic foundations under in-plane loads for various temperatures using the element-free Galerkin (EFG) method based on the first-order shear deformation theory (FSDT). Yu *et al.* [25] studied the buckling and postbuckling behavior of a sandwich plate with a homogeneous core and graphene-reinforced composite face sheets resting on an elastic foundation in thermal environments using the higher order shear deformation plate theory and the von Kármán-type kinematic nonlinearity to derive the governing equations accounting for the plate-foundation interaction and the thermal effects and a two-step perturbation technique for solution. Cong *et al.* [26] presented an analytical approach to investigate buckling and post-buckling behavior of the FGM plate with porosities resting on elastic foundations and subjected to mechanical, thermal and thermomechanical loads. The formulations are based on Reddy's higher-order shear deformation plate theory taking into consideration the von Kármán nonlinearity, initial geometrical imperfections, and the Pasternak type of elastic foundations. Shahrestani [27] investigated elastic buckling of square and skew thin functionally graded material (FGM) plates with a cutout resting on an elastic foundation simulated by the Winkler and two-parameter Pasternak using the isoparametric spline finite strip method. Gupta and Talha [28] investigated the static and stability characteristics of the geometrically imperfect functionally graded material (FGM) plate with a microstructural defect (porosity) resting on the Pasternak elastic foundation. Moita *et al.* [29, 30] presented the formulation for linear buckling and for the geometrically nonlinear analysis of laminated composite and functionally graded material (FGM) plates under mechanical uniaxial in-plane uniform loads and thermal loads. Do and Lee [31] presented an isogeometric analysis (IGA) for investigating the buckling behavior of functionally graded material (FGM) plates in thermal environments using the new $n$-th order shear deformation theory with the von Kármán type of geometric nonlinearity with the optimum order number to best approximate the thermal buckling problem. Sobhy and Zenkour [32] developed a new quasi-3D refined plate theory to study mechanical buckling and free vibration analyses of double-porous functionally graded (FG) nanoplates embedded in the elastic foundation. Singh and Harsha [33] investigated buckling responses of the functionally graded material (FGM) plate subjected to uniform, linear, and non-linear in-plane loads developing a new nonlinear in-plane load models based on the trigonometric and exponential function.

Do *et al.* [34] introduced a mesh-free approximation based on the radial point interpolation method (RPIM) to predict the post-buckling responses of FGM plates in mechanical edge compression using the higher-order shear deformation theory in which a new hybrid type transverse shear function was incorporated. Liu *et al.* [35] analysed thermo-mechanical buckling of porous FGM beams with the porosity caused by manufacturing defects based on the neutral surface. Zenkour and Radwan [36] investigated the effect of exponential temperature and moisture concentration on the bending and buckling analysis of functionally graded plates resting on two-parameter elastic foundations via a four-variable exponential shear deformation theory using the Navier method. Taczała, Buczkowski and Kleiber have already investigated stability of the FGM plates in the elastic [37, 38] and elastic-plastic range [39].

In the present paper we develop a procedure for the buckling and postbuckling analysis of the FGM plates resting on the two-parameter Vlasov elastic foundation using the third order plate theory originally formulated by Reddy and Kim [40] and modified by Taczała *et al.* [41]. A key parameter governing the behaviour of the elastic foundation is evaluated iteratively, following the iterative method given by Vallabhan and Daloglu [42].

## 2. Mathematical formulation

### 2.1. General third-order plate theory

Various deformation theories have been developed for plates. The drawbacks of the classical plate theory and the first-order shear deformation theory (FSDT) are well-known and have been thoroughly discussed in the literature. These problems can be overcome applying higher-order shear deformation plate theories

(HSDT) which offer accurate solutions and allow to avoid problems related to first-order theories. The HSDT use higher order polynomials in the expansion of the displacement components through the thickness of the plate allowing for warping of the cross section. Unlike the FSDT, the HSDT require no shear correction factors. Examples here are the general third-order theory with tangential traction free surfaces or the Reddy third-order theory. These theories, however, have certain drawbacks related to the fact that their formulations require the $C^0$-interpolation for $u_m, v_m, \theta_x, \theta_y$ and the Hermite interpolation for $w_m, \theta_z, \varphi_z$. Moreover, in some cases these theories result in unsymmetrical finite element stiffness matrices even for a linear case [40]. The problem related to various interpolations was addressed by PANDYA and KANT [43] who proposed a method of developing an isoparametric displacement finite element formulation including the conditions for vanishing of the transverse shear partly during defining the displacement field as well as when formulating the shear rigidity matrix and used it for the laminated composite plates. REDDY and KIM [40] proposed the formulation free from the described limitations. The displacement field for the general third-order plate theory (GTPT) is:

$$
\begin{aligned}
u(x, y, z) &= u_m(x, y) + z\theta_x(x, y) + z^2\varphi_x(x, y) + z^3\psi_x(x, y), \\
v(x, y, z) &= v_m(x, y) + z\theta_y(x, y) + z^2\varphi_y(x, y) + z^3\psi_y(x, y), \\
w(x, y, z) &= w_m(x, y) + z\theta_z(x, y) + z^2\varphi_z(x, y).
\end{aligned} \tag{2.1}
$$

Assuming the in-plane displacements $u$, $v$ in the form of the cubic polynomial and the out-of-plane displacement $w$ in the quadratic polynomial with respect to $z$ we obtain a quadratic variation of the transverse shear in this direction with all the displacements contributing to this distribution. The formulation was employed to derive the equations of motion with the use of the modified couple stress theory for FGM plates. The same formulation was also presented for the analysis of the bending deflections of FGM plates [44]. In both cases the von Kármán nonlinear strains were considered. A similar approach has also been proposed by the other authors [45, 46].

In Eq. (2.1) we have eleven generalized displacements: displacements at the mid-surface $u_m, v_m, w_m$, rotations of the transverse normal $\theta_x, \theta_y$ as well as higher order displacements which have more complex physical interpretation $\theta_z$, $\varphi_x$, $\varphi_y$, $\varphi_z$, $\psi_x$, $\psi_y$. For instance, $\theta_z$ is a constant term in the expression for strain $\varepsilon_z$ (and the total strain at the mid-surface):

$$
\varepsilon_z = \left.\frac{\partial w}{\partial z}\right|_{z=0} = \theta_z, \tag{2.2}
$$

while $\varphi_z$ is a multiplier of the linear term of the strain variation

$$
\frac{\partial \varepsilon_z}{\partial z} = \frac{\partial^2 w}{\partial z^2} = 2z\varphi_z. \tag{2.3}
$$

The assumed displacement field given by Eq. (2.1) allows for the parabolic variation of transverse shear strains. The cubic variation of in-plane displacements causes the transverse normal to deteriorate from the straight form while the quadratic variation of out-of-plane displacement implies extension through the thickness thus leading to varying thickness of the plate and emerging direct stresses in the direction of $z$ coordinate.

### 2.2. Modelling of FGM plates

The FGM plate with a top ceramic surface ($c$) and a bottom metal ($m$) surface is assumed. The continuous change of volume fraction of ceramic $V_c$ and metal $V_m$ through the plate thickness is described by the power law

$$V_c = \left(\frac{1}{2} + \frac{z}{t}\right)^n \qquad (n \geq 0), \tag{2.4}$$

where $n$ is the power-law exponent and $z \in \left[-\frac{t}{2}, \frac{t}{2}\right]$ is a coordinate in the thickness direction. Gradation is modelled by an appropriate choice of exponent $n$; assumption of $n = 0$ gives the fully ceramic fraction and $n \to \infty$ gives the fully metal fraction.

The rule of mixture is used to calculate the effective Young modulus $E_f(z)$ in the lamina of FGM

$$E_f = E_m V_m + E_c V_c, \tag{2.5}$$

where $E_c$ and $E_m$ are the material properties of ceramic and metal constituents, respectively. The constant value of the Poisson ratio $\nu$ is assumed, since the effect of its variation on the results is negligible [47].

### 2.3. Modelling of FGM plates

In analysis of structures resting on the elastic foundation, the Winkler model is introduced in which it can be modelled by the row of elastic springs which do not affect each other. Only one parameter $k_0$ is used to describe the foundation behaviour. FILONENKO-BORODICH [48] and PASTERNAK [49] managed to do Winkler model a more realistic postulating a two-parameter model. Their model takes into account the effect of shear interaction. In this model the shear parameter has to be determined experimentally. VLASOV and LEONTIEV [50] have introduced another arbitrary parameter, $\gamma$, dependent on foundation material and thickness of the foundation layer and suggested an approximate value of $\gamma$ between 1 and 2. However, they did not report the method of determining this parameter. In the paper of VALLABHAN and DALOGLU [42], it has been shown how the foundation parameter, $\gamma$, can be estimated iteratively.

Two foundation models can be formulated: linear and quadratic. For the first case, the elastic foundation modulus $E_F(z)$ is a linear function of the through-thickness coordinate $z$

$$E_F(z) = E_{F1} + (E_{F2} - E_{F1})\frac{z}{h}, \tag{2.6}$$

where $E_{F1}$ and $E_{F2}$ are the elasticity modules at the top and bottom of the foundation, respectively, and $h$ is the foundation thickness.

In the paper of Celik and Omurtag [51] a quadratic version of elasticity modulus $E_F(z)$ is formulated

$$E_F(z) = E_{F1} + (E_{F2} - E_{F1})\frac{z^2}{h^2}. \tag{2.7}$$

The two parameters $k_0$ and $k_1$ in terms of the elastic constants and the dimensions of the foundation have been introduced by Vlasov and Leontiev [50]. These parameters applied to a foundation with a finite depth of foundation, $h$, are defined by:

$$k_0 = \frac{E_0}{1-\nu_0^2}\int_0^h \psi'(z)^2 \,\mathrm{d}z \tag{2.8}$$

and

$$k_1 = \frac{E_0}{2(1+\nu_0)}\int_0^h \psi^2(z) \,\mathrm{d}z \tag{2.9}$$

with the mode function $\psi(z)$ which can be obtained using variational principles and applying the proper boundary conditions, such as $\psi(0) = 1$ and $\psi(h) = 0$ as shown in [52], where the following mode function was proposed:

$$\psi(z) = \frac{\sinh\gamma\frac{h-z}{h}}{\sinh\gamma}. \tag{2.10}$$

The generalized modulus of elasticity, $E_0$, and the Poisson ratio, $\nu_0$, are defined by:

$$E_0 = \frac{E_F}{1-\nu_F^2}, \qquad \nu_0 = \frac{\nu_F}{1-\nu_F}, \tag{2.11}$$

where $E_F$ and $\nu_F$ are the modulus of elasticity and the Poisson ratio of the foundation, respectively. If the elasticity modulus $E_S(z)$ is constant through the thickness of the foundation and using the mode function $\psi(z)$ as given in Eq. (2.10), the foundation parameters $k_0$ (Eq. (2.8) and $k_1$ (Eq. (2.9)) become:

$$k_0 = \frac{E_F(1-\nu_F)}{8h(1+\nu_F)(1-2\nu_F)} \frac{2\gamma \sinh(2\gamma) + 4\gamma^2}{\sinh^2 \gamma} \tag{2.12}$$

and

$$k_1 = \frac{E_F h}{16\gamma^2(1+\nu_F)} \frac{2\gamma \sinh(2\gamma) - 2\gamma^2}{\sinh^2 \gamma}. \tag{2.13}$$

However, these parameters also depend on a coefficient $\gamma$, which represents the rate of decrease of the displacement and the normal stresses in the vertical direction in the foundation. According to [52] the parameter $\gamma$ can be evaluated as

$$\gamma^2 = h^2 \frac{1-\nu_F}{2(1-\nu_F)} \frac{\int_{-\infty}^{+\infty}\int_{-\infty}^{+\infty} \left\{ \left(\frac{\partial w(x,y)}{\partial x}\right)^2 + \left(\frac{\partial w(x,y)}{\partial y}\right)^2 \right\} \mathrm{d}x\,\mathrm{d}y}{\int_{-\infty}^{+\infty}\int_{-\infty}^{+\infty} w^2(x,y)\,\mathrm{d}x\,\mathrm{d}y}, \tag{2.14}$$

which can be calculated using an iterative computational process as it is dependent on displacements.

For the foundation in which the modulus $E_F$ can vary linearly in the vertical direction from $E_1$ at the top ($z = 0$) to $E_2$ at the bottom ($z = h$) – Eq. (2.6), expressions for the foundation parameters $k_0$ and $k_1$ can be modified to the following form:

$$k_0 = \frac{1-\nu_F}{8h(1+\nu_F)(1-2\nu_F)} \times \frac{[E_1(2\gamma \sinh(2\gamma) + 4\gamma^2) + (E_2 - E_1)(\cosh(2\gamma) - 1 + 4\gamma^2)]}{\sinh^2 \gamma} \tag{2.15}$$

and

$$k_1 = \frac{h}{16\gamma^2(1+\nu_F)} \times \frac{[E_1(2\gamma \sinh(2\gamma) - 2\gamma^2) + (E_2 - E_1)(\cosh(2\gamma) - 1 - 2\gamma^2)]}{\sinh^2 \gamma}. \tag{2.16}$$

When the elasticity modulus $E_F(z)$ changes quadratically through the depth of the foundation – Eq. (2.7), the parameters $k_0$ and $k_1$ change to:

$$k_0 = \frac{1-\nu_F}{24h\gamma(1+\nu_F)(1-2\nu_F)} \times \frac{3[E_2 + E_1(2\gamma^2 - 1)]\sinh(2\gamma) + 2\gamma[E_2(4\gamma^2 - 3) + E_1(3 + 2\gamma^2)]}{\sinh^2 \gamma} \tag{2.17}$$

and

$$k_1 = \frac{h}{48\gamma^3(1+\nu_F)} \times \frac{3[E_2 + E_1(2\gamma^2 - 1)]\sinh(2\gamma) - 2\gamma[E_2(4\gamma^2 + 3) + E_1(2\gamma^2 - 3)]}{\sinh^2 \gamma}. \tag{2.18}$$

### 2.4. Derivation of incremental finite element equations

Nonlinear finite element equations in the incremental formulation are derived using the principle of virtual work which for increment $t+\Delta t$ and iteration $i+1$ is given by

$$\delta\,{}^{t+\Delta t}_{i+1}W_{int} = \delta\,{}^{t+\Delta t}_{i+1}W_{ext}, \tag{2.19}$$

where $\delta\,{}^{t+\Delta t}_{i+1}W_{ext}$ is the virtual work of external forces for an increment $t+\Delta t$ and iteration $i+1$

$$\delta\,{}^{t+\delta t}_{i+1}W_{ext} = \int\limits_V {}^{t+\delta t}_{i+1}b_i\,\delta\,{}^{t+\Delta t}_{i+1}u_i\mathrm{d}V + \int\limits_\Omega {}^{t+\delta t}_{i+1}p_i\,\delta\,{}^{t+\delta t}_{i+1}u_i\,\mathrm{d}\Omega. \tag{2.20}$$

In Eq. (2.20) $\{{}^{t+\delta t}_{i+1}b_i\}$ is the vector of the body forces acting in volume $V$ (increment $t+\Delta t$, iteration $i+1$), $\{{}^{t+\delta t}_{i+1}p_i\}$ is the loading distributed over area $\Omega$, while $\{{}^{t+\delta t}_{i+1}u_i\}$ denotes the displacement functions dependent on the formulation corresponding to either the plate theory or the solid formulation.

Virtual work of internal forces (2$^{\mathrm{nd}}$ Piola–Kirchhoff stresses) $\delta\,{}^{t+\Delta t}_{i+1}W_{int}$ is the sum of work for the plate and elastic foundation:

$$\delta\,{}^{t+\Delta t}_{i+1}W_{int} = \delta\,{}^{t+\Delta t}_{i+1}W^{(P)}_{int} + \delta\,{}^{t+\Delta t}_{i+1}W^{(F)}_{int}, \tag{2.21}$$

where

$$\delta\,{}^{t+\Delta t}_{i+1}W^{(P)}_{int} = \int\limits_V {}^{t+\Delta t}_{i+1}\sigma_{ij}\,\delta\,{}^{t+\Delta t}_{i+1}\Delta\varepsilon_{ij}\,\mathrm{d}V \tag{2.22}$$

and, using the model of the elastic foundation

$$\begin{aligned}\delta\,{}^{t+\Delta t}_{i+1}W^{(F)}_{int} &= \int\limits_A k_0\,{}^{t+\Delta t}_{i+1}w\,\delta\,{}^{t+\Delta t}_{i+1}w\,\mathrm{d}A\\ &+ \int\limits_A k_1\big[{}^{t+\Delta t}_{i+1}\gamma_{xz}\,\delta\,{}^{t+\Delta t}_{i+1}\gamma_{xz} + {}^{t+\Delta t}_{i+1}\gamma_{yz}\,\delta\,{}^{t+\Delta t}_{i+1}\gamma_{yz}\big]\,\mathrm{d}A.\end{aligned} \tag{2.23}$$

Increments of the Green–Lagrange strains $\{{}^{t+\Delta t}_{i+1}\Delta\varepsilon_{ij}\}$ assuming large displacements can be derived using von Kármán nonlinear strain–displacement relations. Applying the finite element approximation and introducing strain-displacement matrices, $[{}^{t+\Delta t}_{i}B^{(1)}_{ijk}]$ and $[{}^{t+\Delta t}_{i}B^{(2)}_{ijkl}]$, the increments of the strains, are given by

$${}^{t+\Delta t}_{i+1}\Delta\varepsilon_{ij} = {}^{t+\Delta t}_{i}B^{(1)}_{ijk}\,{}^{t+\Delta t}_{i+1}\Delta d_k + {}^{t+\Delta t}_{i}B^{(2)}_{ijkl}\,{}^{t+\Delta t}_{i+1}\Delta d_k\,{}^{t+\Delta t}_{i+1}\Delta d_l, \tag{2.24}$$

where $\{{}^{t+\Delta t}_{i+1}\Delta d_k\}$ are increments of the nodal displacements. We also note that ${}^{t+\Delta t}_{i+1}\gamma_{xz} = 2{}^{t+\Delta t}_{i+1}\varepsilon_{13}$, ${}^{t+\Delta t}_{i+1}\gamma_{yz} = 2{}^{t+\Delta t}_{i+1}\varepsilon_{23}$, therefore, the expression for the virtual work can be written in the incremental form as:

$$\begin{aligned}\delta{}^{t+\Delta t}_{i+1}W_{int} = &\int\limits_V \big({}^{t+\Delta t}_{i}\sigma_{ij} + {}^{t+\Delta t}_{i+1}\Delta\sigma_{ij}\big)\delta{}^{t+\Delta t}_{i+1}\Delta\varepsilon_{ij}\,\mathrm{d}V \\ &+ \int\limits_A k_0({}^{t+\Delta t}_{i}w + {}^{t+\Delta t}_{i+1}\Delta w)\delta{}^{t+\Delta t}_{i+1}\Delta w\,\mathrm{d}A \\ &+ 4\int\limits_A k_1\big[({}^{t+\Delta t}_{i}\varepsilon_{13} + \Delta{}^{t+\Delta t}_{i+1}\varepsilon_{13})\delta\Delta{}^{t+\Delta t}_{i+1}\varepsilon_{13} \\ &+ ({}^{t+\Delta t}_{i}\varepsilon_{23} + \Delta{}^{t+\Delta t}_{i+1}\varepsilon_{23})\delta\Delta{}^{t+\Delta t}_{i+1}\varepsilon_{23}\big]\,\mathrm{d}A.\end{aligned} \tag{2.25}$$

The stress increments are evaluated using the constitutive relationship

$${}^{t+\Delta t}_{i+1}\Delta\sigma_{ij} = {}^{t+\Delta t}_{i}D_{ijkl}\,{}^{t+\Delta t}_{i+1}\Delta\varepsilon_{kl}. \tag{2.26}$$

The principle of virtual work using Eqs. (2.20)–(2.26) takes the form:

$$\begin{aligned}&\int\limits_V {}^{t+\Delta t}_{i}D_{ijkl}\,{}^{t+\Delta t}_{i}B^{(1)}_{klq}\,{}^{t+\Delta t}_{i}B^{(1)}_{ijp}\,{}^{t+\Delta t}_{i+1}\Delta d_q\,\mathrm{d}V \\ &+ \int\limits_V {}^{t+\Delta t}_{i}\sigma_{ij}\big({}^{t+\Delta t}_{i}B^{(2)}_{ijpq} + {}^{t+\Delta t}_{i}B^{(2)}_{ijqp}\big){}^{t+\Delta t}_{i+1}\Delta d_q\,\mathrm{d}V + \int\limits_A k_0 N_{3q}N_{3p}\,\mathrm{d}A \\ &+ 4k_1\int\limits_A\Big\{\big[{}^{t+\Delta t}_{i}B^{(1)}_{13q}\,{}^{t+\Delta t}_{i}B^{(1)}_{13p} + {}^{t+\Delta t}_{i}\varepsilon_{13}\big({}^{t+\Delta t}_{i}B^{(2)}_{13pq} + {}^{t+\Delta t}_{i}B^{(2)}_{13qp}\big)\big] \\ &+ {}^{t+\Delta t}_{i}B^{(1)}_{23q}\,{}^{t+\Delta t}_{i}B^{(1)}_{23p} + {}^{t+\Delta t}_{i}\varepsilon_{23}\big({}^{t+\Delta t}_{i}B^{(2)}_{23pq} + {}^{t+\Delta t}_{i}B^{(2)}_{23qp}\big)\Big\}\,\mathrm{d}A\,{}^{t+\Delta t}_{i+1}\Delta d_q \\ =&\int\limits_V {}^{t+\delta t}_{i+1}b_i N_{ip}\,\mathrm{d}V + \int\limits_\Omega {}^{t+\delta t}_{i+1}p_i N_{ip}\,\mathrm{d}\Omega - \Big[\int\limits_V {}^{t+\Delta t}_{i}\sigma_{ij}\,{}^{t+\Delta t}_{i}B^{(1)}_{ijp}\,\mathrm{d}V \\ &+ \int\limits_A k_0\,{}^{t+\Delta t}_{i}w N_{3p}\,\mathrm{d}A + 4\int\limits_A k_1\big({}^{t+\Delta t}_{i}\varepsilon_{13}\,{}^{t+\Delta t}_{i}B^{(1)}_{13p} + {}^{t+\Delta t}_{i}\varepsilon_{23}\,{}^{t+\Delta t}_{i}B^{(1)}_{23p}\big)\,\mathrm{d}A\Big],\end{aligned} \tag{2.27}$$

what can be written as

$$\big({}^{t+\Delta t}_{i}K^{(P-d)}_{pq} + {}^{t+\Delta t}_{i}K^{(P-\sigma)}_{pk} + {}^{t+\Delta t}_{i}K^{(F)}_{pq}\big){}^{t+\Delta t}_{i+1}\Delta d_q = P^{(P)}_p - F^{(P)}_p + F^{(F)}_p, \tag{2.28}$$

where

$${}^{t+\Delta t}_{i}K^{(P-d)}_{pq} = \int\limits_V {}^{t+\Delta t}_{i}D_{ijkl}\,{}^{t+\Delta t}_{i}B^{(1)}_{klq}\,{}^{t+\Delta t}_{i}B^{(1)}_{ijp}\,{}^{t+\Delta t}_{i+1}\Delta d_q\,\mathrm{d}V \tag{2.29}$$

is the plate stiffness matrix dependent on displacements (including also the linear term)

$$(2.30)\qquad {}^{t+\Delta t}_{i}K^{(P-\sigma)}_{pk} = \int_V {}^{t+\Delta t}_{i}\sigma_{ij}\left({}^{t+\Delta t}_{i}B^{(2)}_{ijpq} + {}^{t+\Delta t}_{i}B^{(2)}_{ijqp}\right){}^{t+\Delta t}_{i+1}\Delta d_q\,\mathrm{d}V$$

is the plate stiffness matrix dependent on stresses,

$$(2.31)\qquad \begin{aligned} {}^{t+\Delta t}_{i}K^{(F)}_{pq} &= \int_A k_0 N_{3q}N_{3p}\,\mathrm{d}A \\ &+ 4k_1\int_A\Big\{\left[{}^{t+\Delta t}_{i}B^{(1)}_{13q}\,{}^{t+\Delta t}_{i}B^{(1)}_{13p} + {}^{t+\Delta t}_{i}\varepsilon_{13}\left({}^{t+\Delta t}_{i}B^{(2)}_{13pq} + {}^{t+\Delta t}_{i}B^{(2)}_{13qp}\right)\right] \\ &+ {}^{t+\Delta t}_{i}B^{(1)}_{23q}\,{}^{t+\Delta t}_{i}B^{(1)}_{23p} + {}^{t+\Delta t}_{i}\varepsilon_{23}\left({}^{t+\Delta t}_{i}B^{(2)}_{23pq} + {}^{t+\Delta t}_{i}B^{(2)}_{23qp}\right)\Big\}\,\mathrm{d}A\,{}^{t+\Delta t}_{i+1}\Delta d_q \end{aligned}$$

is the foundation stiffness matrix,

$$(2.32)\qquad P^{(P)}_p = \int_V {}^{t+\delta t}_{i+1}b_i N_{ip}\,\mathrm{d}V + \int_\Omega {}^{t+\delta t}_{i+1}p_i N_{ip}\,\mathrm{d}\Omega$$

is the reference load vector,

$$(2.33)\qquad F^{(P)}_p = \int_V {}^{t+\Delta t}_{i}\sigma_{ij}\,{}^{t+\Delta t}_{i}B^{(1)}_{ijp}\,\mathrm{d}V$$

is the internal force vector resulting from the plate stresses, and

$$(2.34)\qquad \begin{aligned} F^{(F)}_p &= \int_A k_0\,{}^{t+\Delta t}_{i}w N_{3p}\,\mathrm{d}A \\ &+ 4\int_A k_1\left({}^{t+\Delta t}_{i}\varepsilon_{13}\,{}^{t+\Delta t}_{i}B^{(1)}_{13p} + {}^{t+\Delta t}_{i}\varepsilon_{23}\,{}^{t+\Delta t}_{i}B^{(1)}_{23p}\right)\mathrm{d}A \end{aligned}$$

is the vector equivalent to an internal force vector, resulting from deflections of the elastic foundation.

The buckling stress (bifurcation point) is found from the condition

$$(2.35)\qquad \det\left({}^{t+\Delta t}_{i}K^{(P-d)}_{pq} + {}^{t+\Delta t}_{i}K^{(P-\sigma)}_{pk} + {}^{t+\Delta t}_{i}K^{(F)}_{pq}\right) = 0.$$

The structural response in the post-buckling regime was analyzed applying the path-following technique in the form of the Crisfield constant arc-length method by adopting a constraint condition in addition to the equation set. The constraint delimiting the displacement increment in each load step ${}^{t+\Delta t}_{i+1}\Delta\mathbf{d}_{incr}$ is expressed by

$$(2.36)\qquad \left({}^{t+\Delta t}_{i+1}\Delta\mathbf{d}_{incr}\right)^T\,{}^{t+\Delta t}_{i+1}\Delta\mathbf{d}_{incr} = \Delta l^2.$$

## 3. Numerical examples

### 3.1. Verification of the formulation

The presented formulation has been verified comparing the obtained results with those available in the literature. For the present model of elastic foundation there are no examples of FGM plates available therefore the example of homogenous plate was used. Çelik and Saygun [53] and Vallabhan *et al.* [52], and Buczkowski and Torbacki [54] analysed a plate of size $9.144 \times 12.192$ m and thickness of $t = 0.1524$ m resting on a non-homogeneous layered soil medium with properties varying linearly in the vertical direction. Their model included the boundary conditions at the bottom of the foundation and the boundary conditions resulting from the symmetry of the structure as 1/4 of the overall plate and foundation was modelled. The problems of rectangular plate on two-parameter foundation subjected to uniformly distributed patch loading have been solved in these references by different methods. Vallabhan *et al.* [52] developed a finite element Vlasov model for rectangular plates resting on an elastic layered soil medium. They performed calculations for different values of $E_2/E_1$ $(1, 2, 3, 10)$ where the foundation parameters $k_0$ and $k_1$ are assumed to be dependent on material properties and the depth of the foundation as well as on the dimensionless parameter $\gamma$ given by Eq. (2.14).

The same case but for homogenous foundation was also studied by Çelik and Saygun [53] and Buczkowski and Torbacki [54]. The calculations were performed for four depths of the foundation, $h = 3.048, 6.096, 9.144$ and $15.24$ m, the Young modulus $E_p = 20685000\,\mathrm{kN/m^2}$ and $E_f = 68950\,\mathrm{kN/m^2}$, the Poisson ratio $\nu_p = 0.20$ and $\nu_f = 0.25$ and for the plate and elastic foundation, respectively. The finite element model is composed of sixteen 16-noded plate elements, employing the Gauss–Lobatto integration scheme, originally presented

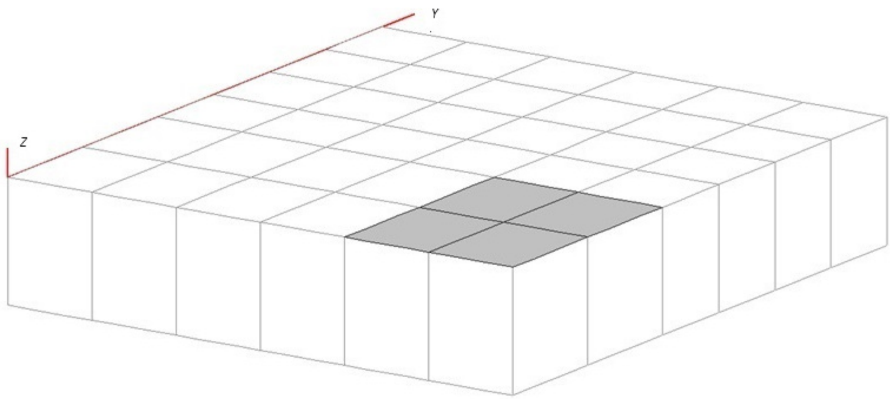


Fig. 1. Finite element model and loading of plate on elastic foundation.

by BUCZKOWSKI *et al.* [55] and sixteen 32-noded zero-thickness foundation elements, based on the concept developed by BUCZKOWSKI and TORBACKI [54]. The boundary conditions are applied to the nodes situated at the bottom of the foundation. The model is presented in Fig. 1 where the nodes coinciding with the integration points as well as the patch loading are visible. The plates are represented by the shaded fragment with the applied loading.

The results of the present calculations are compared with those reported by VALLABHAN *et al.* [52] and ÇELIK and SAYGUN [53] (see Table 1) and it can be concluded that the agreement is good. As seen in the table, the parameter $k_0$ decreases as $t$ increases while the parameter $k_1$ increases with $t$. We can see that the plate deflections increase with the depth of the foundation.

TABLE 1. Vertical displacement at centre of plate for uniformly distributed load.

| $h$ [m] | Method | $\gamma$ | $k_0$ [kN/m$^3$] | $k_1$ [kN/m] | $w_{Centr}$ [cm] |
|---|---|---|---|---|---|
| 3.048 | VALLABHAN *et al.* [52] | 0.5766 | 27192 | 26826 | 0.0853 |
| | ÇELIK and SAYGUN [53] | 0.5724 | 27206 | 26904 | 0.0872 |
| | BUCZKOWSKI and TORBACKI [54], 3 × 3 Gauss | 0.5724 | 27207 | 26852 | 0.0871 |
| | present | **0.5650** | **27204** | **26881** | **0.0873** |
| 6.096 | VALLABHAN *et al.* [52] | 0.9297 | 13757 | 50282 | 0.1524 |
| | ÇELIK, SAYGUN [53] | 0.9194 | 13757 | 50410 | 0.1526 |
| | BUCZKOWSKI and TORBACKI [54], 3 × 3 Gauss | 0.9194 | 13758 | 50411 | 0.1530 |
| | present | **0.9148** | **13754** | **50462** | **0.1521** |
| 9.144 | VALLABHAN *et al.* [52] | 1.2644 | 9430 | 69506 | 0.1890 |
| | ÇELIK and SAYGUN [53] | 1.2064 | 9377 | 70586 | 0.1893 |
| | BUCZKOWSKI and TORBACKI [54], 3 × 3 Gauss | 1.2064 | 9378 | 50587 | 0.1896 |
| | present | **1.1832** | **9356** | **71014** | **0.1853** |
| 15.24 | VALLABHAN *et al.* [52] | 1.9419 | 6366 | 94732 | 0.2070 |
| | ÇELIK and SAYGUN [53] | 1.6193 | 5964 | 104664 | 0.2212 |
| | BUCZKOWSKI and TORBACKI [54], 3 × 3 Gauss | 1.6193 | 5964 | 104664 | 0.2205 |
| | present | **1.4887** | **5835** | **108790** | **0.2067** |

### 3.2. Buckling and post-buckling of axially compressed homogenous plates

We begin with the analysis of the bifurcation buckling. To illustrate the buckling and post-buckling a homogenous plate was analysed. The dimensions of the plate were taken as follows: 800 × 800 mm, thickness $t = 16$ mm, elastic foundation 1600 × 1600 mm, depth $h = 50$ mm. Material properties were the Young modulus of the plate $E_p = 207780\,\mathrm{N/mm^2}$, and the foundation $E_f = 207.7$, the Poison ratio $\nu_p = 0.3177$ and $\nu_f = 0.25$ for the plate and foundation, respectively. Boundary conditions were taken to model the symmetry of the structure and the structural response. We note that this condition includes not only translational displacements and rotations but also components of the displacement functions of higher orders, not having direct physical interpretation: $\varphi_x$, $\varphi_y$, $\psi_x$, $\psi_y$ as explained in the section on the formulation of the applied plate theory. Regarding the solid elements modelling the foundation the nodes belonging solely to them have single DOF – vertical displacement. This DOF is blocked at the bottom of the foundation whereas remains free at the top. Loading is implemented as mechanical compression of one of the plate edges in the model (Fig. 2).

The response of the plate in the form of loading vs. deflection of the central node is given in Fig. 3. The buckling mode is presented in Fig. 4.

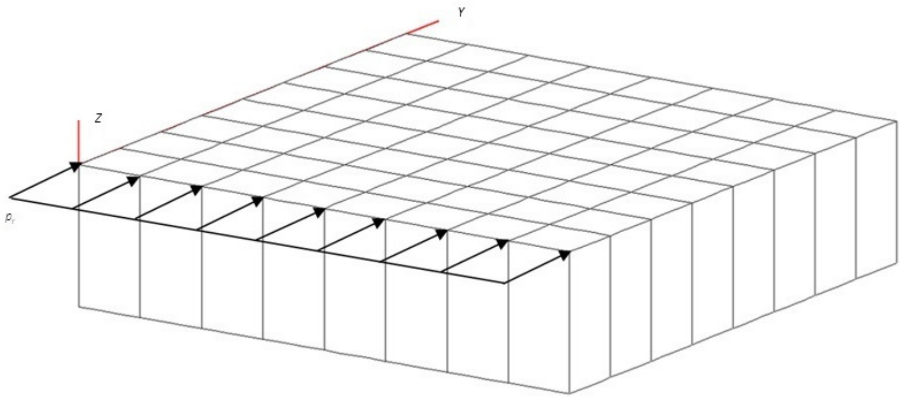


Fig. 2. Finite element model and compressive loading of plate on elastic foundation.

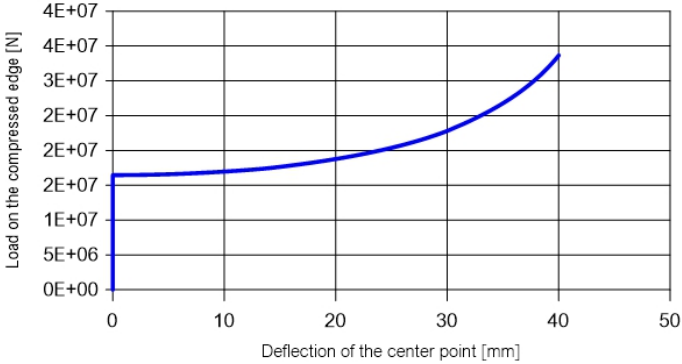


Fig. 3. Loading of compressed edge vs. deflection of central node for bifurcation buckling.

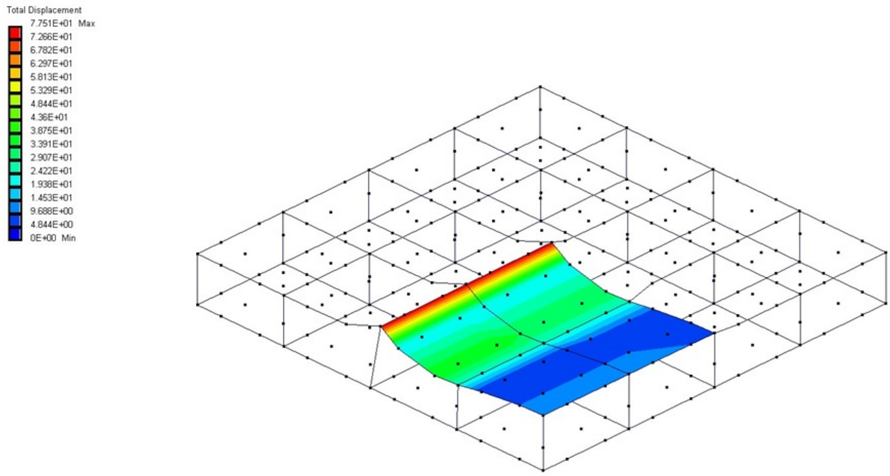


Fig. 4. Buckling mode in case of bifurcation buckling.

### 3.3. Buckling and post-buckling of axially compressed FGM plates

Influence of various parameters on buckling and post-buckling behaviour of FGM plates positioned on the elastic foundation is presented here for the square plate having dimensions as previously in the case of homogenous plate; $a \times a = 800 \times 800$ mm, elastic foundation $1600 \times 1600$ mm. Material properties in all cases were taken as the following: the Young modulus of the metallic part $E_m = 207780$ MPa, the Young modulus of the ceramic part $E_c = 322270$ MPa, the Poisson ratio of both ceramic and metallic parts $v_c = v_m = 0.3177$. The Poisson ratio of the elastic foundation was taken equal to $\nu_f = 0.25$. Similarly to the model of the homogenous plate, the boundary conditions were taken to model the symmetry of the structure and the structural response, as were introduced the boundary conditions for the solid elements modelling the foundation. All other parameters: the Young modulus of the elastic foundation, exponent of the power-law, plate thickness, depth of the elastic foundation and type of the distribution of the foundation modulus throughout the depth – linear and quadratic vary in the analysed examples. We note, that the behaviour of the FGM plates subject to the compression applied uniformly on the area delimiting the plate is similar to the behaviour of the plate with initial deflection that is the response curve (loading vs. deflection) is smooth and the buckling stress cannot be unambiguously identified (the effect can be seen in the following Figs. 5–11). Therefore commenting the results term "buckling stress" is referred to the level of stress (loading) for the specific value of deflection, to enable comparison between various curves.

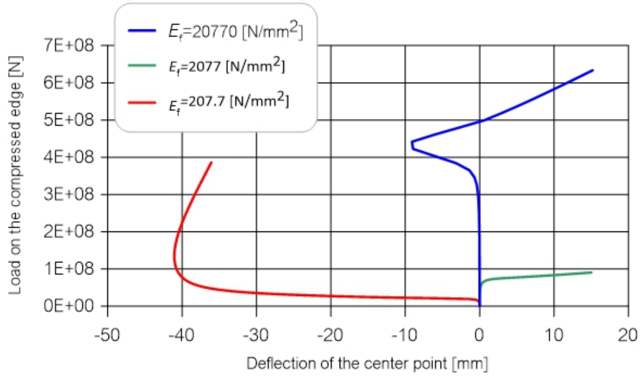


FIG. 5. Influence of Young modulus of elastic foundation on buckling and post-buckling behaviour of compressed square plate.

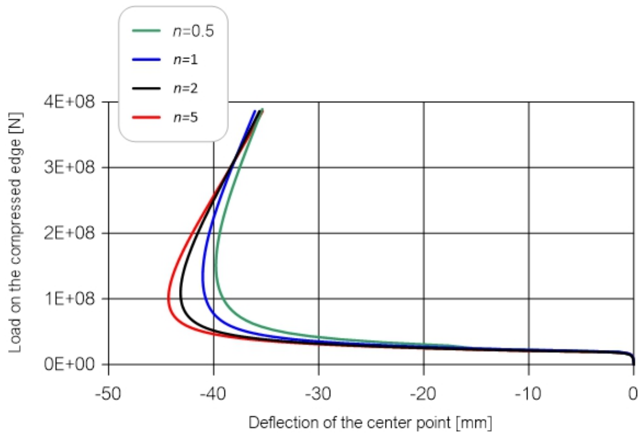


FIG. 6. Influence of exponent in the power law on buckling and post-buckling behaviour of compressed square plate.

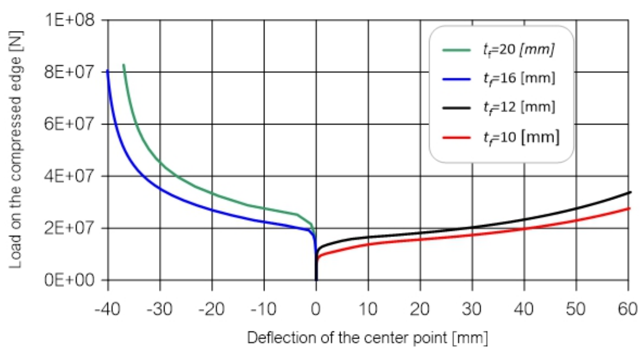


FIG. 7. Influence of plate thickness on buckling and post-buckling behaviour of compressed square plate.

In Fig. 5 we can see the influence of the Young modulus of the elastic foundation (constant throughout the depth) for the plate $t = 16$ mm, exponent $n = 1$, foundation depth $t_f = 50$ mm. The Young modulus of the elastic foundation varies from 207.7 N/mm$^2$ (1/100 of the nominal value equal to 20770 N/mm$^2$) to the nominal value. The influence is significant and the buckling stress increases in fact proportionally to the increase of the Young modulus of the elastic foundation. Moreover, we can observe different curves for various values of the Young modulus.

Influence of exponent in the power law $n$ (Eq. (2.4)) is presented in Fig. 6. This time we can see almost identical values of the buckling stress and similar behaviour with small difference in maximum deflection of the centre point.

In Fig. 7 we observe an increasing buckling stress with the increasing plate thickness which is a fairly obvious effect. An unpredictable thing is that the buckling modes are different – in the positive direction for thinner plates ($t_p = 10$ and 12 mm) and in negative for thicker plates ($t_p = 16$ and 20 mm).

Explanation of the behaviour of the situation is presented in Figs. 8 and 9 where the buckling modes of plates on the elastic foundation are presented.

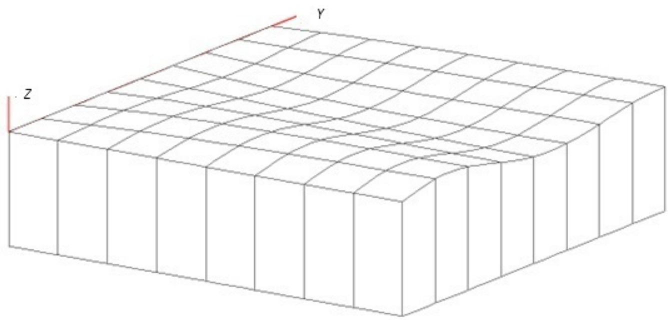


FIG. 8. Buckling mode for compressed square plate of thickness $t_p = 12$ mm.

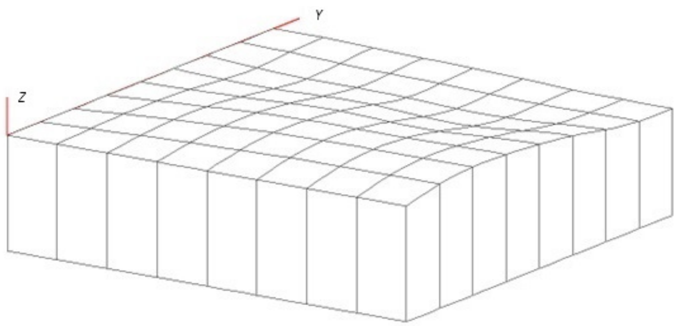


FIG. 9. Buckling mode for compressed square plate of thickness $t_p = 16$ mm.

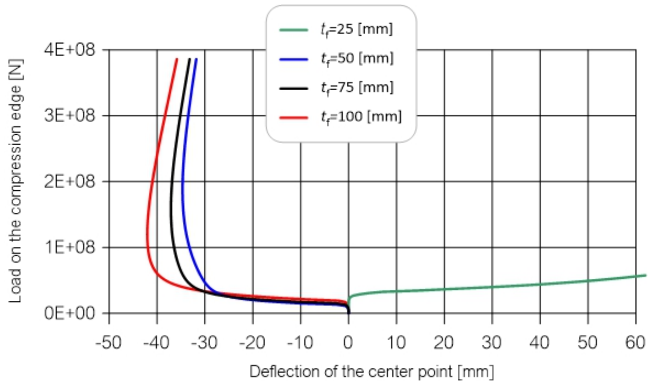


Fig. 10. Influence of foundation depth on buckling and post-buckling behaviour of compressed square plate.

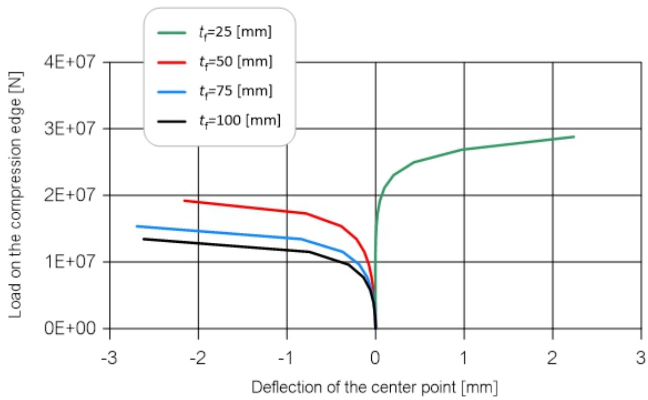


Fig. 11. Influence of foundation depth on buckling and post-buckling behaviour of compressed square plate – initial part of response.

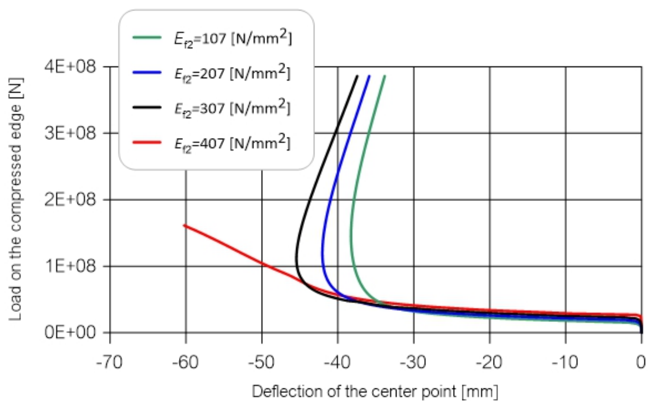


Fig. 12. Influence of Young modulus at bottom on buckling and post-buckling behaviour of compressed square plate for linear type of distribution.

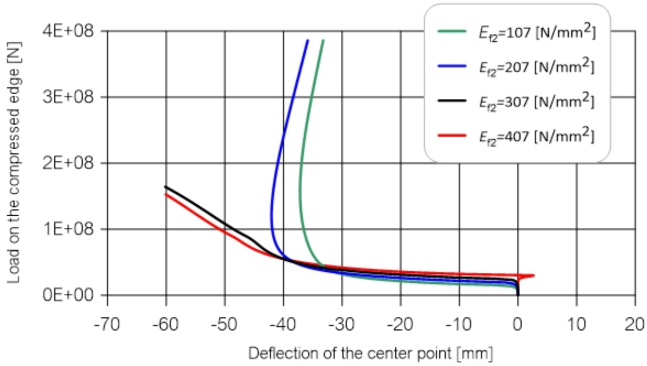


Fig. 13. Influence of Young modulus at bottom on buckling and post-buckling behaviour of compressed square plate for quadratic type of distribution.

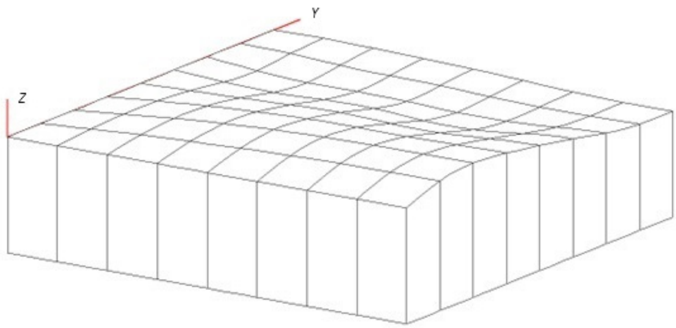


Fig. 14. Buckling mode for compressed square plate, linear type of distribution of Young modulus of elastic foundation, $E_{f1} = 107\,\mathrm{N/mm^2}$ and $E_{f2} = 207\,\mathrm{N/mm^2}$.

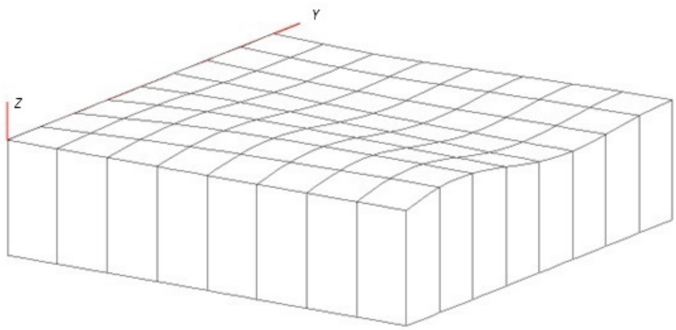


Fig. 15. Buckling mode for compressed square plate, linear type of distribution of Young modulus of elastic foundation, $E_{f1} = 107\,\mathrm{N/mm^2}$ and $E_{f2} = 307\,\mathrm{N/mm^2}$.

A similar situation is also seen in Figs. 9 and 10 where the structural response is visualized for various depths of the elastic foundation. This time we receive positive deflection for $t_f = 25\,\mathrm{mm}$, while for the greater values we have negative.

The buckling stress in the case of various depths is reduced with the increase of the thickness of the elastic foundation.

The influence of the type of the distribution of the Young modulus – value at the top of the foundation $E_{f1} = 207\,\mathrm{N/mm^2}$ and $E_{f2}$ ranging from 107 to $407\,\mathrm{N/mm^2}$ in all cases, the difference is that the linear distribution of the Young modulus was taken to produce the results presented in Fig. 12 while the quadratic distribution – in Fig. 13. The curves are similar in both figures except for $E_{f2} = 407\,\mathrm{N/mm^2}$ (linear distribution of the Young modulus) as well as $E_{f2} = 307$ and $407\,\mathrm{N/mm^2}$ (quadratic distribution of the Young modulus) the responses are entirely different. It is, as in the case of the investigation of the influence of the plate thickness the reason is in different buckling modes for various Young modulus of the foundation – Figs. 14 and 15.

## 4. Conclusions

Analysis of buckling and nonlinear behaviour of functionally graded material (FGM) plates resting on the elastic foundation has been presented. The generalized third-order plate theory and the Vlasov formulation were used for modelling plates resting on the elastic foundation having properties varying throughout the depth. The formulation was verified against the results available in the literature. Several examples presenting influence of various parameters on behaviour of compressed plates – including buckling and post-buckling – were presented. The following specific conclusions can be formulated based on the analysis:

1. Buckling stress:
   - is strongly dependent on the Young modulus of the elastic foundation,
   - is insensitive to the exponent in the power law,
   - decreases with an increasing depth of the elastic foundation.
2. The structural response is dependent not only on the material properties of the plate and elastic foundation but also on the type of distribution of the Young modulus of the elastic foundation throughout its depth.

## Acknowledgements

The work has been performed under the project functionally graded materials-static and dynamic analyses, financed by the Polish National Science Centre (NCN) under the contract 2018/29/B/ST8/02723. The support is gratefully acknowledged.

## References


1. K. Swaminathan, D.T. Naveenkumar, A.M. Zenkour, E. Carrera, *Stress, vibration and buckling analyses of FGM plates – A state-of-the-art review*, Composite Structures, **120**, 10–31, 2015, doi: 10.1016/j.compstruct.2014.09.070.
2. K. Swaminathan, D.M. Sangeetha, *Thermal analysis of FGM plates – A critical review of various modeling techniques and solution methods*, Composite Structures, **160**, 43–60, 2017, doi: 10.1016/j.compstruct.2016.10.047.
3. A. Hassan Ahmed Hassan, N. Kurgan, *A Review on buckling analysis of functionally graded plates under thermo-mechanical loads*, International Journal of Engineering and Applied Sciences, **11**, 1, 345–368, 2019, doi: 10.24107/ijeas.555719.
4. K. Swaminathan, D.T. Naveenkumar, *Higher order refined computational models for the stability analysis of FGM plates – Analytical solutions*, European Journal of Mechanics – A/Solids, **47**, 349–361, 2014, doi: 10.1016/j.euromechsol.2014.06.003.
5. R. Javaheri, M.R. Eslami, *Buckling of functionally graded plates under in-plane compressive loading*, ZAMM-Zeitschrift für Angewandte Mathematik und Mechanik, **82**, 4, 277–283, 2002, doi: 10.1002/1521-4001(200204)82:4<277::AID-ZAMM277>3.0.CO;2-Y.
6. B.A. Samsam-Shariat, M.R. Eslami, *Buckling of thick functionally graded plates under mechanical and thermal loads*, Composite Structures, **78**, 3, 433–439, 2007, doi: 10.1016/j.compstruct.2005.11.001.
7. T. Prakash, M.K. Singha, M. Ganapathi, *Thermal postbuckling analysis of FGM skew plates*, Engineering Structures, **30**, 1, 22–32, 2008, doi: 10.1016/j.engstruct.2007.02.012.
8. T. Prakash, M. Singha, M. Ganapathi, *Influence of neutral surface position on the nonlinear stability behavior of functionally graded plates*, Computational Mechanics, **43**, 3, 341–350, 2009, doi: 10.1007/s00466-008-0309-8.
9. M. Aydogdu, *Conditions for functionally graded plates to remain flat under in-plane loads by classical plate theory*, Composite Structures, **82**, 1, 155–7, 2008, doi: 10.1016/j.compstruct.2006.10.004.
10. Y.Y. Lee, X. Zhao, J.N. Reddy, *Post-buckling analysis of functionally graded plates subjected to compressive and thermal loads*, Computer Methods in Applied Mechanics and Engineering, **199**, 25-28, 1645–1653, 2010, doi: 10.1016/j.cma.2010.01.008.
11. A.M. Zenkour, M. Sobhy, *Thermal buckling of various types of FGM sandwich plates*, Composite Structures, **93**, 1, 93–102, 2018, doi: 10.1016/j.compstruct.2010.06.012.
12. N.D. Duc, H. Van Tung, *Mechanical and thermal postbuckling of higher order shear deformable functionally graded plates on elastic foundations*, Composite Structures, **93**, 11, 2874–2881, 2011, doi: 10.1016/j.compstruct.2011.05.017.
13. M. Bodaghi, A.R. Saidi, *Stability analysis of functionally graded rectangular plates under nonlinearly varying in-plane loading resting on elastic foundation*, Archive of Applied Mechanics, **81**, 6, 765–780, 2011, doi: 10.1007/s00419-010-0449-0.
14. A.H. Akbarzadeh, M. Abbasi, M.R. Eslami, *Coupled thermo-elasticity of functionally graded plates based on the third-order shear deformation theory*, Thin-Walled Structures, **53**, 141–155, 2012, doi: 10.1016/j.tws.2012.01.009.
15. K. Kowal-Michalska, R. Mania, *Static and dynamic thermo-mechanical buckling loads of functionally graded plates*, Mechanics and Mechanical Engineering, **17**, 1, 99–112, 2013.

16. D.G. Zhang, *Modeling and analysis of FGM rectangular plates based on physical neutral surface and high order shear deformation theory*, International Journal of Mechanical Sciences, **68**, 92–104, 2013, doi: 10.1016/j.ijmecsci.2013.01.002.

17. M. Latifi, F. Farhatnia, M. Kadkhodaei, *Buckling analysis of rectangular functionally graded plates under various edge conditions using Fourier series expansion*, European Journal of Mechanics – A/Solids, **41**, 16–27, 2013, doi: 10.1016/j.euromechsol.2013.01.008.

18. H.T. Thai, B. Uy, *Levy solution for buckling analysis of functionally graded plates based on a refined plate theory*, Proceedings of the Institution of Mechanical Engineers, Part C: Journal of Mechanical Engineering Science, **12**, 2649–2664, 2013, doi: 10.1177/0954406213478526

19. M.H. Mansouri, M. Shariyat, *Biaxial thermo-mechanical buckling of orthotropic auxetic FGM plates with temperature and moisture dependent material properties on elastic foundations*, Composites Part B: Engineering, **83**, 88–104, 2015, doi: 10.1016/j.compositesb.2015.08.030.

20. S.-C. Han, W.-T. Park, W.-Y. Jung, *Four-variable refined plate theory for dynamic stability analysis of S-FGM plates based on physical neutral surface*, Composite Structures, **131**, 1081–1089, 2015, doi: 10.1016/j.ijmecsci.2016.03.001.

21. Y-H. Lee, S-I. Bae, J-H. Kim, *Thermal buckling behavior of functionally graded plates based on neutral surface*, Composite Structures, **137**, 208–214, 2016, doi: 10.1016/j.compstruct.2015.11.023.

22. Y. Fan, H. Wang, *Nonlinear bending and postbuckling analysis of matrix cracked hybrid laminated plates containing carbon nanotube reinforced composite layers in thermal environments*, Composites Part B: Engineering, **86**, 1–16, 2016, doi: 10.1016/j.compositesb.2015.09.048.

23. A. Chikh, A. Bakora, H. Heireche, M.S.A. Houari, A. Tounsi, E.A. Adda Bedia, *Thermo-mechanical postbuckling of symmetric S-FGM plates resting on Pasternak elastic foundations using hyperbolic shear deformation theory*, Structural Engineering and Mechanics, **57**, 4, 617–639, 2016, doi: 10.12989/sem.2016.57.4.617.

24. S. Shams, B. Soltani, M. Memar Ardestani, *The effect of elastic foundations on the buckling behavior of functionally graded carbon nanotube-reinforced composite plates in thermal environments using a meshfree method*, Journal of Solid Mechanics, **8**, 2, 262–279, 2016.

25. Y. Yu, H.S. Shen, H. Wang, D. Hui, *Postbuckling of sandwich plates with graphene-reinforced composite face sheets in thermal environments*, Composites Part B: Engineering, **135**, 72–83, 2018, doi: 10.1016/j.compositesb.2017.09.045.

26. P.H. Cong, T.M. Chien, N.D. Khoa, N.D. Duc, *Nonlinear thermomechanical buckling and post-buckling response of porous FGM plates using Reddy's HSDT*, Aerospace Science and Technology, **77**, 419–428, 2018, doi: 10.1016/j.ast.2018.03.020.

27. M.G. Shahrestani, M. Azhari, H. Foroughi, *Elastic and inelastic buckling of square and skew FGM plates with cutout resting on elastic foundation using isoparametric spline finite strip method*, Acta Mechanica, **229**, 2079–2096, 2018, doi: 10.1007/s00707-017-2082-2.

28. A. Gupta, M. Talha, *Static and Stability Characteristics of Geometrically Imperfect FGM Plates Resting on Pasternak Elastic Foundation with Microstructural Defect*, The Arabian Journal for Science and Engineering, **43**, 4931–4947, 2018, doi: 10.1007/s13369-018-3240-0.

29. J.S. Moita, A.L. Araújo, V.F. Correia, C.M.M. Soares, *Buckling and nonlinear response of functionally graded plates under thermo-mechanical loading*, Composite Structures, **202**, 719–730, 2018, doi: 10.1016/j.compstruct.2018.03.082.

30. J.S. Moita, A.L. Araújo, V.F. Correia, C.M.M. Soares, *Buckling behavior of composite and functionally graded material plates*, European Journal of Mechanics A/Solids, **80**, 103921, 2020, doi: 10.1016/j.euromechsol.2019.103921.

31. V.N.V. Do, C.H. Lee, *A new nth-order shear deformation theory for isogeometric thermal buckling analysis of FGM plates with temperature-dependent material properties*, Acta Mechanica, **230**, 3783–3805, 2019, doi: 10.1007/s00707-019-02480-1.

32. M. Sobhy, A.M. Zenkour, *Porosity and inhomogeneity effects on the buckling and vibration of double-FGM nanoplates via a quasi-3D refined theory*, Composite Structures, **220**, 289–303, 2019, doi: 10.1016/j.compstruct.2019.03.096.

33. S.J. Singh, S.P. Harsha, *Buckling analysis of FGM plates under uniform, linear and non-linear in-plane loading*, Journal of Mechanical Science and Technology, **33**, 4, 1761–1767, 2019, doi: 10.1007/s12206-019-0328-8.

34. V.N.V. Do, K.H. Chang, C.H. Lee, *Post-buckling analysis of FGM plates under in-plane mechanical compressive loading by using a mesh-free approximation*, Archive of Applied Mechanics, **89**, 1421–1446, 2019, doi: 10.1007/s00419-019-01512-5.

35. Y. Liu, S. Su, H. Huang, Y. Liang, *Thermal-mechanical coupling buckling analysis of porous functionally graded sandwich beams based on physical neutral plane*, Composites Part B-Engineering, **168**, 236–242, 2019, doi: 10.1016/j.compositesb.2018.12.063.

36. A.M. Zenkour, A.F. Radwan, *Bending and buckling analysis of FGM plates resting on elastic foundations in hygrothermal environment*, Archives of Civil and Mechanical Engineering, **20**, 4, 198–220, 2020, doi: 10.1007/s43452-020-00116-z.

37. M. Taczała, R. Buczkowski, M. Kleiber, *Nonlinear free vibration of pre- and post-buckled FGM plates on two-parameter foundation in the thermal environment*, Composite Structures, **137**, 85–92, 2016, doi: 10.1016/j.compstruct.2015.11.017.

38. M. Taczała, R. Buczkowski, M. Kleiber, *Nonlinear buckling and post-buckling response of stiffened FGM plates in thermal environments*, Composites Part B: Engineering, **109**, 238–247, 2017, doi: 10.1016/j.compositesb.2016.09.023.

39. M. Taczała, R. Buczkowski, M. Kleiber, *Elastic-plastic buckling and postbuckling finite element analysis of plates using higher-order theory*, International Journal of Structural Stability and Dynamics, **21**, 7, 2150095, 2021, doi: 10.1142/S0219455421500954.

40. J.N. Reddy, J. Kim, *A nonlinear modified couple stress-based third-order theory of functionally graded plates*, Composite Structures, **94**, 1128–1143, 2012, doi: 10.1590/S1679-78252014000300006.

41. M. Taczała, R. Buczkowski, M. Kleiber, *Analysis of FGM plates based on physical neutral surface using general third-order plate theory*, Composite Structures, **301**, 1–7, 2022, doi: 10.1016/j.compstruct.2022.116218.

42. C.V.G. Vallabhan, A.T. Daloglu, *Consistent FEM-Vlasov model for plates on layered soil*, Journal of Structural Engineering – ASCE, **125**, 10, 108–113, 1999, doi: 10.1061/(ASCE)0733-9445(1999)125:1(108).

43. B.N. Pandya, T. Kant, *A simple finite element formulation of a higher-order theory for unsymmetrically laminated composite plates*, Composite Structures, **9**, 3, 215–246, 1988, doi: 10.1016/0263-8223(88)90015-3.

44. J. Kim, J.N. Reddy, *A general third-order theory of functionally graded plates with modified couple stress effect and the von Kármán nonlinearity: theory and finite element analysis*, Acta Mechanica, **226**, 2973–2998, 2015, doi: 10.1007/s00707-015-1370-y.

45. E. Carrera, *Theories and finite elements for multilayered plates and shells: a unified compact formulation with numerical assessment and benchmarking*, Archives of Computational Methods in Engineering, **10**, 215–296, 2003, doi: 10.1007/BF02736224.

46. A.M.A. Neves, A.J.M. Ferreira, E. Carrera, M. Cinefra, C.M.C. Roque, R.M.N. Jorge, C.M.M. Soares, *Static, free vibration and buckling analysis of isotropic and sandwich functionally graded plates using a quasi-3D higher-order shear deformation theory and a meshless technique*, Composites Part B: Engineering, **44**, 1, 657–674, 2013, doi: 10.1016/j.compositesb.2012.01.089.

47. S-H. Chi, Y-L. Chung, *Mechanical behavior of functionally graded material plates under transverse load Part II: numerical results*, International Journal of Solids and Structures, **43**, 13, 3675–3691, 2006, doi: 10.1016/j.ijsolstr.2005.04.010.

48. M.M. Filonenko-Borodich, *Some approximate theories of elastic foundation.* Uchenyie Zapiski Moskovskogo Gosudarstvennogo Universiteta, Mekhanika, **46**, 3–18, 1940 [in Russian].

49. P.L. Pasternak, *New Method of Calculation for Flexible Substructures on Two-parameter Elastic Foundation*, Gosudarstvennoe Izdatelstvo Literatury po Stroitelstvu i Architekture, Moscow, pp. 1–56, 1954 [in Russian].

50. V.Z. Vlasov, N.N. Leontiev, *Beams, Plates and Shells on Elastic Foundations,* GIFML, Moskau, 1960, [in Russian] or translated from Russian by Foundation: Israel Program for Scientific Translations, Jerusalem, 1966.

51. M. Celik, M. Omurtag, *Determination of the Vlasov foundation parameters-quadratic variation of elasticity modulus using FE analysis*, Structural Engineering and Mechanics, **19**, 6, 619–637, 2005, doi: 10.12989/sem.2005.19.6.619.

52. C.V.G. Vallabhan, W.T. Straughan, Y.C. Das, *Refined model for analysis of plates on elastic foundations*, Journal of Engineering Mechanics – ASCE, **117**, 12, 2830–2844, 1991, doi: 10.1061/(ASCE)0733-9399(1991)117:12(2830).

53. M. Çelik, A. Saygun, *A method for the analysis of plates on a two-parameter foundation*, International Journal of Solids and Structures, **36,** 19, 2891–2915, 1999, doi: 10.1016/S0020-7683(98)00135-8.

54. R. Buczkowski, W. Torbacki, *Finite element modelling of thick plates on two-parameter elastic foundation*, International Journal of Numerical and Analytical Methods in Geomechanics, **25**, 14, 1409–1427, 2001, doi: 10.1002/nag.187.

55. R. Buczkowski, M. Taczała, M. Kleiber, *A 16-node locking-free Mindlin plate resting on two-parameter elastic foundation – static and eigenvalue analysis*, Computer Assisted Methods in Engineering and Science, **22**, 2, 99–114, 2015.

*Received February 27, 2024; revised version July 8, 2024.*

*Published online October 8, 2024.*